Boosting Organic Pollutants Degradation by Surface Defects of Iron Oxide Nanofibers

Yingying Ma, Yijing Liu

Abstract

The discharge of organic dyes poses a significant challenge to water resources and environmental quality, highlighting the critical importance of developing efficient catalysts for their degradation. In this study, iron (III) oxide nanofibers were synthesized via electrospinning method and high-temperature calcination, followed by the construction of oxygen vacancy defects on the surface of the nanofibers through the method of reduction using $NaBH_4$. The results indicate that the presence of oxygen vacancy defects substantially enhances the catalytic activity of the nanofibers in degrading organic dyes such as methylene blue and rhodamine B. These optimized properties not only position iron (III) oxide as a highly effective material in the field of organic dye degradation but also offer valuable insights for the structural design of high-performance degradation catalysts, contributing significantly to water resource protection and sustainable development.

Key words: pollutants degradation, defects, iron oxide nanofiber, oxygen vacancy

Content

Abstract **2**

1. Introduction **4**

2. Experimental Section **6**

2.1 Preparation of Iron Oxide Nanofibers and Construction of Surface Defects 6

2.2 Structural Characterization of Catalytic performance 6

2.3 Catalytic Oxidative Degradation of Organic Dyes 7

3. Results and discussion **7**

4. Conclusion **15**

Reference **16**

1. Introduction

Organic dyes such as methylene blue (MB) and rhodamine B (RhB) are widely used in industrial production[1, 2]. However, the wastewater from these processes contains a significant amount of undecomposed dye molecules and other organic pollutants, characterized by high chromaticity and chemical reactivity. When industrial dye wastewater is discharged, the organic substances it contains may infiltrate the soil, affecting soil fertility and biodiversity, and may even enter groundwater systems, leading to groundwater contamination[3]. Effectively treating industrial dye wastewater is crucial for protecting the environment and human health[4, 5]. Consequently, the development and application of environmentally friendly dyes and efficient wastewater treatment technologies have become increasingly important[6]. Common treatment methods include biodegradation[7], catalytic oxidation[8], photocatalysis[9], ion exchange[10], and membrane separation[11] technologies. These approaches can effectively degrade and remove harmful substances from dye wastewater, thereby reducing its environmental impact.

Chemical catalytic oxidation is a method that employs catalysts to facilitate oxidation reactions and is widely used in fields such as chemical synthesis, wastewater treatment, and environmental protection[12, 13]. Selecting an appropriate catalyst is crucial in catalytic oxidation. Common catalysts in chemical catalysis include metal catalysts, oxide catalysts, acid-base catalysts, and enzyme catalysts[14, 15]. Among these, transition metal oxide catalysts are particularly important. These catalysts are often employed in oxidation reactions, redox reactions, and catalytic cracking processes[16, 17]. Transition metal oxide catalysts exhibit high activity and selectivity, enabling them to catalyze various complex reactions, such as oxidation, hydrogenation, and oxygen reduction. States of the transition metal elements and the unique properties of their crystal structures. Common transition metal oxide catalysts include iron oxides, cobalt oxides, and nickel oxides[18, 19]. These catalysts play a critical role in industrial applications, such as organic synthesis, environmental protection, and energy conversion[20, 21]. Chemical catalytic oxidation offers numerous advantages. Firstly, catalysts can lower the activation energy of reactions, increase reaction rates, and in some cases, enhance product selectivity, thereby reducing the formation of by-products. Secondly, compared to non-catalytic oxidation reactions, catalytic oxidation typically occurs at lower temperatures and pressures, which reduces energy consumption and operational costs. Additionally, the reusability of

catalysts contributes to their longer service life and reduces waste generation, aligning with the goals of environmental sustainability.

Iron oxide (Fe_2O_3) is a highly favored catalyst due to its numerous advantages. Iron oxide exhibits excellent catalytic activity, enabling it to facilitate many important chemical reactions such as oxidation, hydrogenation, and catalytic cracking[22, 23]. The catalyst demonstrates good stability under various conditions, maintaining its catalytic activity over prolonged periods and reducing catalyst deactivation rates. Additionally, iron oxide catalysts are renewable; their catalytic activity can be restored through simple treatments or regeneration processes, thereby extending their lifespan. Compared to some other catalysts, iron oxide is more environmentally friendly, as the raw materials used in its preparation are relatively common and do not pose significant environmental risks[24, 25]. Owing to its superior properties, iron oxide catalysts have been widely applied in fields such as organic synthesis, environmental protection, and energy conversion, providing efficient catalytic performance for a variety of critical reactions.

Oxygen vacancy defects offer significant advantages in catalytic applications by allowing control over catalytic reactions through the modification of the surface structure and chemical properties of the catalyst[26]. This provides new strategies and approaches for designing and developing efficient and selective catalysts. Firstly, oxygen vacancy defects create additional active sites that can adsorb and activate reactant molecules, thereby promoting the progression of the reaction[27]. This increases the contact opportunities between the catalyst surface and the reactants, enhancing the reaction rate. Secondly, oxygen vacancy defects can modulate the electronic structure of the catalyst, altering the interactions between the catalyst and reactants, thus influencing the reaction selectivity[28]. For example, oxygen vacancy defects may partially reduce the catalyst surface, increasing its catalytic activity for reduction reactions. Additionally, oxygen vacancy defects can serve as stabilization sites for reaction intermediates, facilitating the reaction process. Lastly, oxygen vacancy defects are tunable; their formation and distribution can be controlled by adjusting the preparation conditions of the catalyst, allowing for precise regulation of catalytic performance. However, research on oxygen vacancy defects on the surface of iron oxide materials in the oxidation degradation of dyes is relatively limited. This study aims to explore the fabrication of defects on the surface of one-dimensional iron oxide nanofibers to enhance their catalytic performance in degrading organic pollutants, achieving efficient

degradation of organic contaminants, and investigating the potential application of oxygen vacancy defects in the degradation of organic dyes.

2. Experimental Section

2.1 Preparation of Iron Oxide Nanofibers and Construction of Surface Defects

Fe_2O_3 nanofibers were prepared using electrospinning method combined with high-temperature calcination. Initially, 1.5 g of $Fe(acac)_3$, 1.5 g of PAN, and 12 g of DMF were added to a 25 mL conical flask. After heating and stirring at 60°C in an oil bath for 12 hours, a uniform and stable spinning solution was obtained. This solution was then transferred into a 10 mL syringe mounted on a microinjection pump, with a 20G metal needle installed at the syringe tip. During the electrospinning process, an electrostatic voltage of 16 kV was applied, with a collection distance of 20 cm, a temperature control of 25°C ± 2°C, and humidity control of 35% ± 5%. Finally, the PAN/$Fe(acac)_3$ fibers obtained from electrospinning were placed in a high-temperature muffle furnace and subjected to calcination at 500°C for 1 hour in an air atmosphere, with a heating rate of $5^oC \cdot min^{-1}$. After cooling, Fe_2O_3 fibers were obtained.

Oxygen Vacancy (V_O) Defects can be constructed on the surface of Fe_2O_3 nanofibers using the $NaBH_4$ reduction method. Initially, 50 mg of Fe_2O_3 and 25 mL of deionized water were added to a 100 mL beaker and subjected to ultrasonic dispersion for 5 minutes. Subsequently, a certain amount of $NaBH_4$ was added to the beaker while stirring at 500 rpm, and the mixture was stirred continuously for 1 hour. Finally, the sample was centrifuged and washed alternately with anhydrous ethanol and deionized water, and then vacuum dried to obtain Fe_2O_3 containing V_O defects.

2.2 Structural Characterization of Catalytic performance

Scanning electron microscopy (SEM) and transmission electron microscopy (TEM) were used to characterize the microstructure of the catalyst. X-ray diffraction (XRD) was employed to determine the crystalline structure of the catalyst. The specific surface area of the material was measured using a physical adsorption instrument. The electronic structure of the catalyst was

analyzed using electron paramagnetic resonance (EPR) and X-ray photoelectron spectroscopy (XPS).

2.3 Catalytic Oxidative Degradation of Organic Dyes

Typically, 12.5 mg of methylene blue (MB) powder was first dissolved by 30 mL of deionized water and stirred with a glass rod until the powder dissolves. The solution was then transferred to a 250 mL volumetric flask to prepare MB solution with a concentration of 50 mg L^{-1}. The preparation of rhodamine B follows the same procedure, resulting in a 250 mL solution with a concentration of 50mg L^{-1}. Similarly, a 10 mL solution of potassium peroxymonosulfate (PMS) with a concentration of 0.5g L^{-1} was prepared using the same method.

In a typical dye oxidation process, 25.0 mL of the prepared MB solution was first added to a beaker. Then 5.0 mg of catalyst (Fe_2O_3 or Fe_2O_3-Vo) was added to the solution and stirred for 30 minutes to reach adsorption equilibrium. 300 μL of PMS solution was added to the above solution and the reaction was started immediately. 200 μL of samples was taken from the reaction solution every 4 minutes for further analysis by spectrophotometer. The oxidation of RhB was carried out using the same procedure.

3. Results and discussion

After electrospinning and calcination, a red sample was obtained as shown in Fig. 1, which was consistent with the color of iron oxide. The as-synthesized iron oxide was put into water by ultrasonic stirring and the solution was red, and the solution slowly turned black after adding $NaBH_4$ solution, and the solid product was centrifuged, washed, and dried after sufficient reaction for 1 hour to obtain the black sample shown on the right side of Fig. 1, which indicated that the iron oxide surface had been reduced to produce the oxygen vacancies and thus led to the color change.

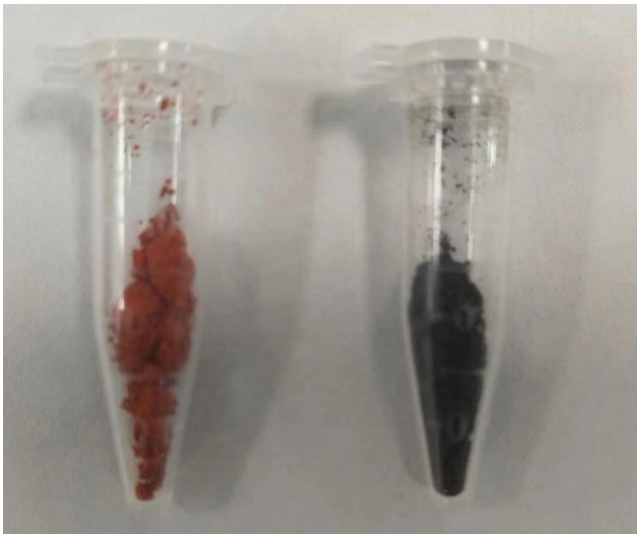

Fig. 1 Digital photographs of the as-synthesized Fe_2O_3 nanofibers (left) and reduced Fe_2O_3 nanofibers with surface oxygen vacancies(right)

The morphology and structure of Fe_2O_3 was characterized and the results are shown in Fig. 2. From the characterization results, it can be found that the Fe_2O_3 obtained after calcination still has a homogeneous morphology (Fig. 2a) with a fibrous structure. The high-magnification cross-sectional SEM image shows that Fe_2O_3 exhibits a thin-walled hollow structure with folds on the surface (Fig. 2b), and the TEM characterization results further confirm the existence of the folds and the thin-walled hollow structure (indicated by arrows in Fig. 2c). The average diameter of Fe_2O_3 nanofiber obtained from statistical calculation was about 608 nm (Fig. 2d). The morphology of Fe_2O_3-V_O obtained after reduction using $NaBH_4$ still maintains the fibrous structure, which is consistent with the morphology of Fe_2O_3 nanofiber before reduction.

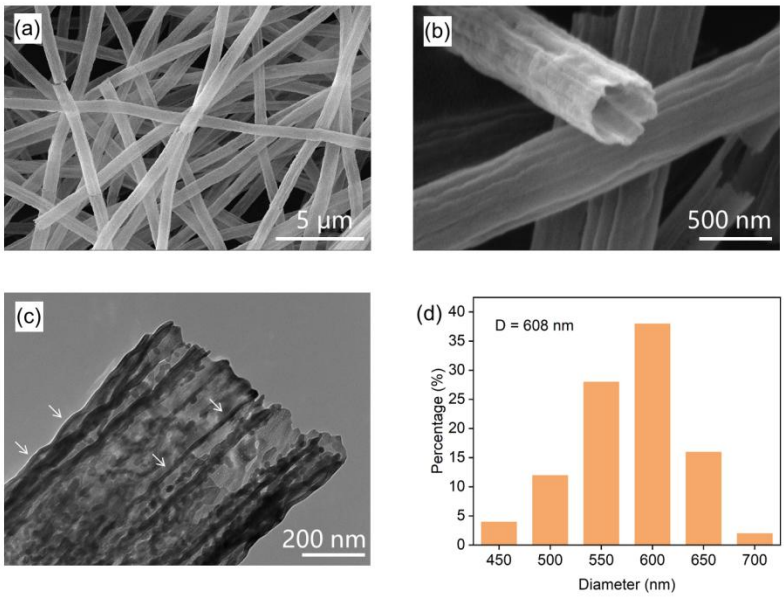

Fig. 2 Morphological characterization and diameter of Fe_2O_3 nanofibers. (a-b) Cross-section SEM images of Fe_2O_3 nanofibers, (c) TEM images of Fe_2O_3 nanofibers, (d) Statistical calculated diameter of Fe_2O_3 nanofibers.

Subsequently, The N_2 adsorption and desorption curves, specific surface area and pore size distribution of Fe_2O_3 were characterized using a physical adsorption instrument, and the results are shown in Fig. 3. Fe_2O_3 showed a type IV adsorption and desorption isomer, with a specific surface area of about 37.99 $m^2 \cdot g^{-1}$, and the pore size distribution was concentrated near 2-3 nm, i.e., the pore structure in Fe_2O_3 was dominated by mesopores. Similarly, the adsorption characteristics of Fe_2O_3-V_O are consistent with those of Fe_2O_3 nanofibers, and the specific surface area does not change significantly.

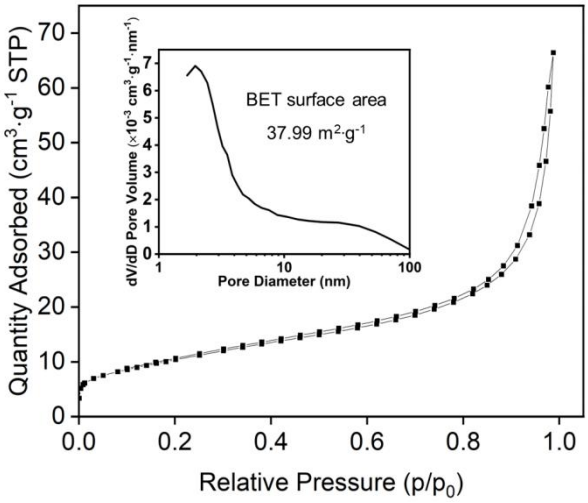

Fig. 3 Specific surface area and pore size distribution of Fe_2O_3 fiber.

X-ray diffraction (XRD) was employed to analyze the crystal phase of Fe_2O_3 nanofibers and Fe_2O_3-V_O, and the results are shown in Fig. 4. From the XRD results, it can be found that both have obvious diffraction peaks at 24.1° (012), 33.2° (104), 35.6° (110), 40.9° (113), and the peak positions of both match with the α- Fe_2O_3 of the Hematite phase (JCPDS No. 33-0664, space group: R-3c)[29], so the construction of the oxygen vacancy defects V_O process did not induce a significant α- Fe_2O_3 phase transition. It should be noted that with the decrease in surface crystallinity induced by the introduction of V_O, the diffraction peak intensities of the Fe_2O_3 -V_O nanofibers show a clear tendency to decrease compared with those of the Fe_2O_3 nanofibers.

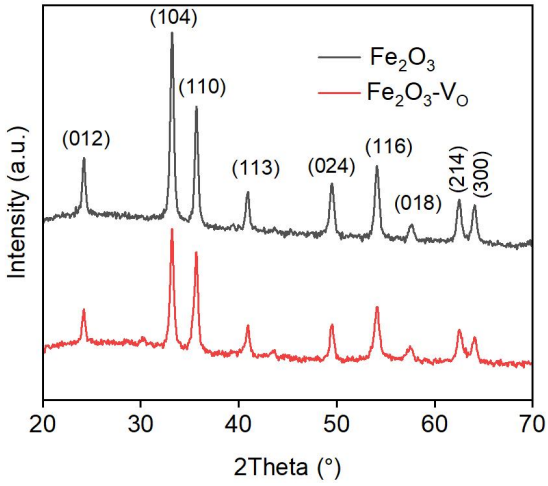

Fig. 4 XRD characterization results of the samples.

EPR was then used to characterize the oxygen vacancy defect V_O. From the characterization results of EPR, it can be seen that the signal near g = 2.002 is that of V_O in Fe_2O_3[30, 31]. Due to the reduction of $NaBH_4$, there is a significant increase in the concentration of V_O in the sample from Fe_2O_3 nanofibers to Fe_2O_3-V_O (Fig. 5). From the figure, it can be seen that a small amount of V_O also exists in the Fe_2O_3 nanofibers, and these oxygen vacancy defects mainly come from the bulk intrinsic defects generated during the calcined PAN/$Fe(acac)_3$ preparation of Fe_2O_3, while the increase in the signal intensity of V_O in Fe_2O_3-V_O is very obvious, indicating that the increase in the concentration of oxygen vacancy defects in Fe_2O_3-V_O is significant, which comes from the $NaBH_4$ reduction process.

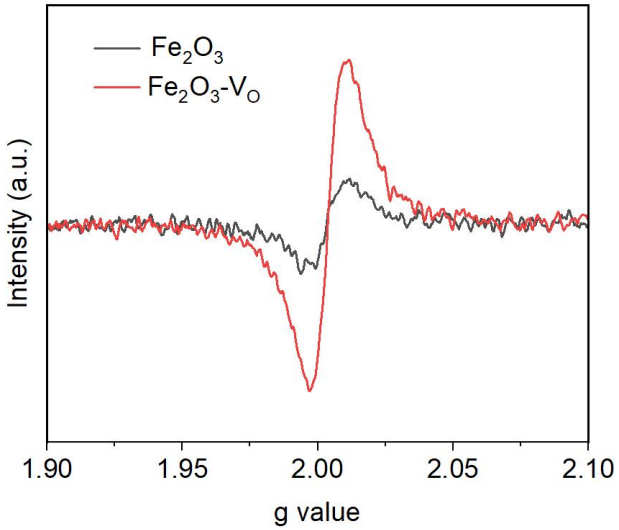

Fig. 5 EPR characterization results of the samples.

Subsequently, X-ray photoelectron spectroscopy (XPS) was employed to further confirm the oxygen vacancy defects. As shown in Fig. 6a, the split-peak fitting results from the O 1s XPS fine spectra of Fe_2O_3 nanofibers and Fe_2O_3-V_O revealed the presence of characteristic peaks in the samples corresponding to O_L (lattice oxygen) species and O_D (defective oxygen) species[32, 33]. In Fe_2O_3 nanofibers, the percentage of O_D is 31.8%, while in Fe_2O_3 -V_O the percentage of O_D increases from 31.8% to 76.6% and the percentage of O_L decreases from 68.2% to 23.4% (Fig. 6), indicating a significant increase in the concentration of V_O in Fe_2O_3 -V_O. This result is also consistent with the results obtained by EPR.

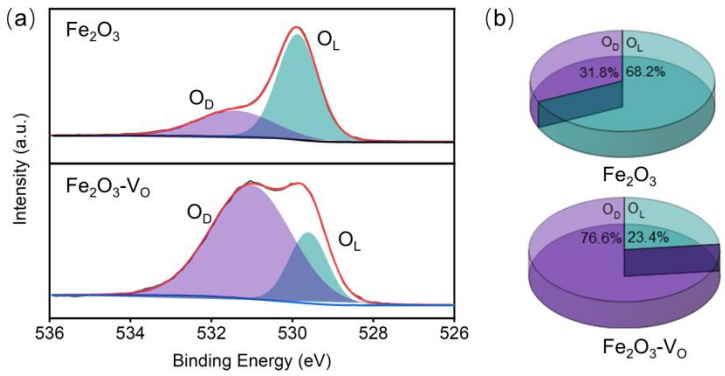

Fig. 6 XPS characterization results of Fe_2O_3 nanofibers and Fe_2O_3-V_O.

Subsequently, Fe2O3 nanofibers and Fe2O3 -VO were applied to the oxidative degradation of two typical organic dyes, MB and RhB. At room temperature, Fe2O3 nanofibers and Fe2O3-VO were added into a solution containing 50 ppm MB and RhB, respectively, and PMS was added as an oxidizing agent. The relative concentration of the two dyes (c/c0) under the action of catalysts as a function of time is shown in Fig. 7. Catalyzed by Fe_2O_3 nanofibers, the concentration of MB decreased slowly with time, and the c/c0 was still about 80% when the reaction was carried out for 16 min, whereas the relative concentration of MB decreases significantly faster with the Fe_2O_3-Vo catalyst, reaching almost zero within the first four minutes, indicating a rapid and complete degradation. This stark difference highlights the superior catalytic performance of Fe_2O_3-Vo, likely due to the presence of oxygen vacancies that enhance the catalytic activity and facilitate a more efficient degradation process of methylene blue compared to the defect-free Fe_2O_3 catalyst. The Fe_2O_3 catalyst with defects thus demonstrates a significantly higher degradation efficiency throughout the experiment, as evidenced by the steeper drop and consistently lower relative concentration of methylene blue. For RhB, similarly, the catalyst with defects (blue line) is more effective in degrading RhB than the catalyst without defects (red line). The defective catalyst reduces the concentration to near-zero by the end of the test period, whereas the non-defective catalyst shows less effective degradation, leaving a higher concentration of dye. The observed differences in degradation efficiency suggest a critical role of oxygen vacancy defects in enhancing the catalytic activity, which warrants a deeper exploration of their impact on the overall performance of the catalyst. The positive role of defects is that the presence of defects in Fe_2O_3 catalysts enhances their degradation capabilities in these cases.

Defects may provide additional active sites or influence the electronic structure in a way that favors the catalytic reaction. This might include the generation of reactive oxygen species or improved adsorption capabilities. In addition to the overall performance, the kinetics of the degradation process provide further insights into the effectiveness and efficiency of the catalysts. It plays rapid initial activity, the steep decline observed initially for both catalysts indicate high activity at the start of the reaction, likely due to abundant active sites and strong adsorption capacity. And it also sustained activity with defects. The catalysts with defects do not show a significant plateau as quickly as their defect-free counterparts, suggesting that they maintain their activity over a longer period, possibly due to a more robust mechanism that utilizes defects effectively.

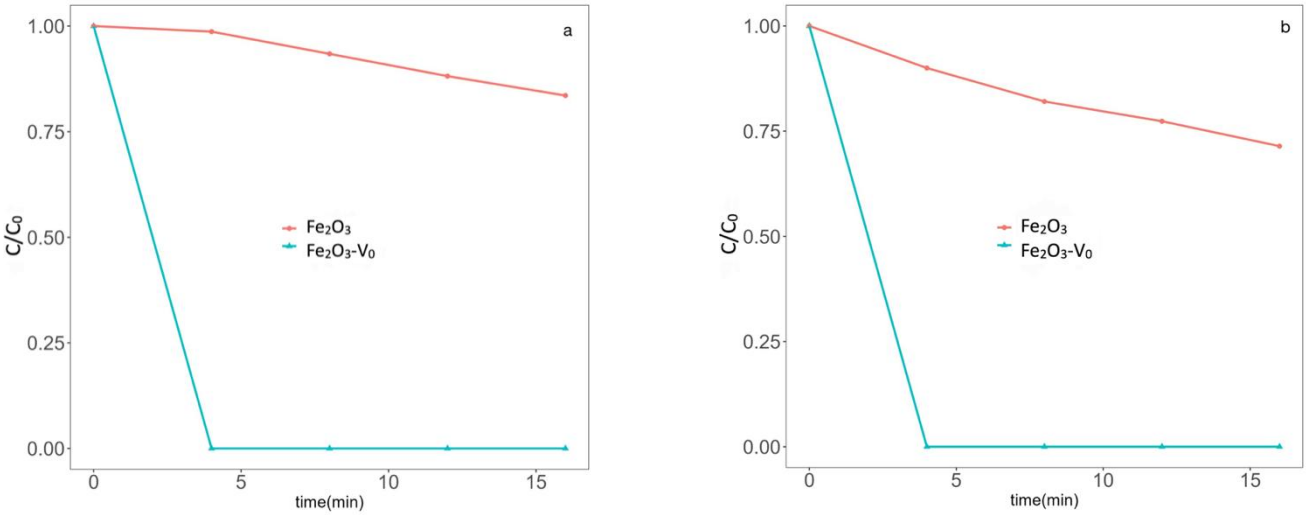

Fig 7. Plot of c/c_0 of reactants as a function of time for Fe_2O_3 nanofibers and Fe_2O_3 -V_O in the catalytic degradation of MB (a) and RhB (b)

To understand the underlying reasons for the enhanced performance of Fe_2O_3-Vo, we examined the potential mechanistic benefits introduced by the defects. The Potential Benefits of Defects is the data suggest that defects may not always be detrimental. They might alter the physical and chemical properties of the catalysts in a way that promotes more efficient degradation of organic pollutants. The Electron and Charge Dynamics is the altered electronic properties due to defects might facilitate better electron transfer processes necessary for catalytic reactions, thereby enhancing the degradation rate. These findings highlight significant implications for the design of future catalysts, particularly in the context of environmental

remediation applications. First is the defect engineering. This observation could lead to targeted engineering of catalysts with specific types of defects to enhance their performance in pollutant degradation. Second is the application in environmental remediation. Catalysts with engineered defects could be particularly useful in applications like wastewater treatment, where efficient and rapid removal of diverse pollutants is required. The presence of defects in Fe_2O_3 catalysts enhances their degradation capabilities in these cases. Defects may provide additional active sites or influence the electronic structure in a way that favors the catalytic reaction. This might include the generation of reactive oxygen species or improved adsorption capabilities. The possible mechanism of Fe_2O_3-V_O accelerating the catalytic degradation of organic dyes by PMS is shown in Fig. 8. The introduction of oxygen vacancy defects will firstly facilitate the adsorption of Fe_2O_3 -V_O on PMS. Secondly, the oxygen vacancies can help electrons to be directly transferred from the organic dyes to the PMS directly, which will lead to the direct degradation of the pollutants; Lastly, the PMS will also be activated by the Fe_2O_3 nanofibers surface of Fe^{3+} /Fe^{2+} to become the more reactive $\cdot SO^{4-}$ and ·OH radicals, which can oxidize the organic pollutants more easily. The presence of oxygen vacancies can change the charge distribution of Fe on the surface of Fe_2O_3 nanofibers and increase the content of Fe^{2+} on the surface, which improves the electron transfer efficiency and promotes the formation of $\cdot SO_4^-$ and ·OH free-radicals.

$$\mathbf{DYE + PMS \xrightarrow[catalyst]{\text{mediated } e^- \text{ transfer}} CO_2 + H_2O + SO_4^{2-}} \quad (1)$$

$$\mathbf{Fe^{2+} + HSO_5^- + V_o \longrightarrow Fe^{3+} + \cdot SO_4^- + H^+} \quad (2)$$

$$\mathbf{Fe^{2+} + HSO_5^- + H_2O + V_o \longrightarrow Fe^{3+} + SO_4^{2-} + \cdot OH + 2H^+} \quad (3)$$

$$\mathbf{Fe^{3+} + HSO_5^- + H^+ \longrightarrow Fe^{2+} + \cdot SO_5^- + H_2O + V_o} \quad (4)$$

$$\mathbf{\cdot SO_4^- / \cdot OH + DYE \longrightarrow intermediates \longrightarrow CO_2 + H_2O} \quad (5)$$

Fig. 8 Schematic diagram of possible processes of Fe_2O_3 catalyzed PMS degradation of organic dyes

4. Conclusion

Fe_2O_3 nanofiber was produced by electrospinning method and high-temperature calcination. Oxygen vacancy defects were further constructed on the surface of Fe_2O_3 nanofibers by $NaBH_4$ reduction to obtain Fe_2O_3-Vo. The formation of oxygen vacancy defects was confirmed by characterization methods, such as XRD, EPR and XPS. Fe_2O_3-Vo with oxygen vacancy defects showed much better catalytic performance when used as catalyst in the oxidative degradation of organic dyes such as MB and RhB, indicating that the oxygen vacancy defect structure can help the activation of PMS for the efficient oxidative degradation of organic dyes. This finding provides a reference for the structural design of catalysts for the degradation of organic pollutants. This study underscores the importance of defect engineering in enhancing the catalytic efficiency of iron oxide nanofibers.

Reference

[1] Xiao, Z.; Wu, R.; Shu, T.; Wang, Y.; Li, L., Synthesis of Co-Doped Fe Metal–Organic Framework MIL-101(Fe,Co) and Efficient Degradation of Organic Dyes in Water. Sep. Purif. Technol. 2023, 304, 122300.

[2] Ding, J.; Pan, Y.; Li, L.; Liu, H.; Zhang, Q.; Gao, G.; Pan, B., Synergetic Adsorption and Electrochemical Classified Recycling of Cr(VI) and Dyes in Synthetic Dyeing Wastewater. Chem. Eng. J. 2020, 384, 123232.

[3] Yu, X.; Zhang, J.; Chen, Y.; Ji, Q.; Wei, Y.; Niu, J.; Yu, Z.; Yao, B., Ag-Cu_2O Composite Films with Enhanced Photocatalytic Activities for Methylene Blue Degradation: Analysis of the Mechanism and the Degradation Pathways. Journal of Environmental Chemical Engineering 2021, 9, 106161.

[4] Fan, L.; Su, X.; Zhu, H.; Liu, H.; Lou, S.; Shi, Y.; Yan, S., Degradation of Methylene Blue by Hot Electrons Transfer in Snse. Adv. Mater. Interfaces 2023, 10, 2202207.

[5] Kong, L.-H.; Wu, Y.; Shen, R.-F.; Zhang, W.-J.; Dong, Z.-Y.; Ge, W.-T.; Guo, X.-J.; Yan, X.; Chen, Y.; Lang, W.-Z., Combination of N-Doped Porous Carbon and g-C_3N_4 for Effective Removal of Organic Pollutants via Activated Peroxymonosulfate. Journal of Environmental Chemical Engineering 2022, 10, 107808.

[6] Chen, Q.; Ning, S.; Yang, J.; Wang, L.; Yin, X.; Wang, X.; Wei, Y.; Zeng, D., In Situ Interfacial Engineering of CeO_2/Bi_2WO6 Heterojunction with Improved Photodegradation of Tetracycline and Organic Dyes: Mechanism Insight and Toxicity Assessment. Small 2023, 20, 2307304.

[7] Rahimi, A.; Alihosseini, F., In Vivo and in Vitro Decolorization of Disperse Azo Dyes Using. Journal of Environmental Engineering 2024, 150, 04024041.

[8] Moumen, A.; Belhocine, Y.; Sbei, N.; Rahali, S.; Ali, F. A. M.; Mechati, F.; Hamdaoui, F.; Seydou, M., Removal of Malachite Green Dye from Aqueous Solution by Catalytic Wet Oxidation Technique Using Ni/Kaolin as Catalyst. Molecules 2022, 27, 7528.

[9] Cong, S.; Cai, J.; Li, X.; You, J.; Wang, L.; Wang, X., Direct Z-Scheme Xylan-Based Carbon Dots@TiO_{2-X} Nanocomposites for Visible Light Driven Photocatalytic of Dye Degradation and Antibacterial. Adv. Funct. Mater. 2024, 34, 2401540.

[10] Yanardağ, D.; Edebali, S., Adsorptive Removal of Malachite Green Dye from Aqueous Solution by Ion Exchange Resins. Biomass Conversion and Biorefinery 2023, 14, 5699.

[11] Ye, H.; Chen, D.; Li, N.; Xu, Q.; Li, H.; He, J.; Lu, J., Polymer of Intrinsic Microporosity Coated on a Metal-Organic Framework Composite Membrane for Highly Efficient Dye Separation. J. Membrane Sci. 2021, 637, 119619.

[12] Zheng, H.; Lu, H.; Li, S.; Niu, J.; Leong, Y. K.; Zhang, W.; Lee, D.-J.; Chang, J.-S., Recent Advances in Electrospinning-Nanofiber Materials Used in Advanced Oxidation Processes for Pollutant Degradation. Environ. Pollut. 2024, 344, 123223.

[13] He, Z.; Ong, J. H.; Bao, Y.; Hu, X., Chemocatalytic Ceramic Membranes for Removing Organic Pollutants in Wastewater: A Review. Journal of Environmental Chemical Engineering 2023, 11, 109548.

[14] Yin, K.; Shang, Y.; Chen, D.; Gao, B.; Yue, Q.; Xu, X., Redox Potentials of Pollutants Determining the Dominate Oxidation Pathways in Manganese Single-Atom Catalyst (Mn-Sac)/Peroxymonosulfate System: Selective Catalytic Mechanisms for Versatile Pollutants. Appl. Catal. B: Environ. 2023, 338, 123029.

[15] Liu, H.; Li, X.; Zhang, X.; Coulon, F.; Wang, C., Harnessing the Power of Natural Minerals: A Comprehensive Review of Their Application as Heterogeneous Catalysts in Advanced Oxidation Processes for Organic Pollutant Degradation. Chemosphere 2023, 337, 139404.
[16] Fumoto, E.; Sato, S.; Takanohashi, T., Characterization of an Iron-Oxide-Based Catalyst Used for Catalytic Cracking of Heavy Oil with Steam. Energ. Fuel. 2018, 32, 2834.
[17] Yang, H.; Li, G.; Jiang, G.; Zhang, Z.; Hao, Z., Heterogeneous Selective Oxidation over Supported Metal Catalysts: From Nanoparticles to Single Atoms. Appl. Catal. B: Environ. 2023, 325, 122384.
[18] Khan, W. U.; Hantoko, D.; Bakare, I. A.; Al Shoaibi, A.; Chandrasekar, S.; Hossain, M. M., Co-Ni on Zirconia and Titania Catalysts for Methane Decomposition to Hydrogen and Carbon Nanomaterials: The Role of Metal-Support Interactions. Fuel 2024, 369, 131675.
[19] Yoon, W.; Jo, H.; Ahmed, S.; Khan, M. K.; Irshad, M.; Lee, J.; Bibi, S. S.; Kim, J., Role of Alkali Metal in Maintaining Iron Integrity During Direct CO_2 Hydrogenation. Chem. Eng. J. 2024, 495, 153617.
[20] Xie, C.; Niu, Z.; Kim, D.; Li, M.; Yang, P., Surface and Interface Control in Nanoparticle Catalysis. Chem. Rev. 2020, 120, 1184.
[21] Li, Z.; Ji, S.; Liu, Y.; Cao, X.; Tian, S.; Chen, Y.; Niu, Z.; Li, Y., Well-Defined Materials for Heterogeneous Catalysis: From Nanoparticles to Isolated Single-Atom Sites. Chem. Rev. 2020, 120, 623.
[22] Geng, Y.; Lian, Z.; Zhang, Y.; Liu, J.; Jin, D.; Shan, W., Heteropoly Acid-Grafted Iron Oxide Catalysts for Efficient Selective Catalytic Reduction of NO_x with NH_3. Catalysis Science & Technology 2024, 14, 3064.
[23] Guo, S.; Yu, Y.; Liu, H.; Gu, M.; Chen, J.; Yao, H., Insight the SCR Mechanism of Selenium Poisoning on α-Fe_2O_3 Catalyst Surface:Experimental and DFT Study. Fuel 2024, 371, 131903.
[24] Guo, S.; Wang, X.; Chen, W.; Xu, J.; Jiang, H., Enhancing Degradation of Sulfapyridine by Magnetic Fe_2O_3-$CoFe_2O_4$@NC Prepared through a Facile Solid Phase Coordination-Calcination Method for Peroxymonosulfate Activation. Chem. Eng. J. 2024, 489, 151204.
[25] Chen, J.; Zhu, B.; Song, W.; Sun, Y., Catalytic Performance of Calcined Fe_2O_3/CA Catalyst for NH_3-SCR Reaction: Role of Activation Temperature. J. Solid State Chem. 2022, 316, 123630.
[26] Chung, C.-H.; Tu, F.-Y.; Chiu, T.-A.; Wu, T.-T.; Yu, W.-Y., Critical Roles of Surface Oxygen Vacancy in Heterogeneous Catalysis over Ceria-Based Materials: A Selected Review. Chem. Lett. 2021, 50, 856.
[27] Wu, Y.; Ma, L.; Wu, J.; Song, M.; Wang, C.; Lu, J., High-Surface Area Mesoporous Sc_2O_3 with Abundant Oxygen Vacancies as New and Advanced Electrocatalyst for Electrochemical Biomass Valorization. Adv. Mater. 2024, 36, e2311698.
[28] Liu, S.-S.; Fu, H.; Wang, F.; Wei, Y.; Meng, B.; Wang, P.; Zhao, C.; Liu, W.; Wang, C.-C., Insight into the Extremely Different Catalytic Behaviors of Asymmetric and Symmetric Oxygen Vacancies for Peroxymonosulfate Activation. Appl. Catal. B: Environ. 2024, 346, 123753.
[29] Sun, J.; Xia, W.; Zheng, Q.; Zeng, X.; Liu, W.; Liu, G.; Wang, P., Increased Active Sites on Irregular Morphological α-Fe_2O_3 Nanorods for Enhanced Photoelectrochemical Performance. ACS Omega 2020, 5, 12339.
[30] Zhang, N.; Li, X.; Liu, Y.; Long, R.; Li, M.; Chen, S.; Qi, Z.; Wang, C.; Song, L.; Jiang, J.; Xiong, Y., Defective Tungsten Oxide Hydrate Nanosheets for Boosting Aerobic Coupling of

Amines: Synergistic Catalysis by Oxygen Vacancies and Bronsted Acid Sites. Small 2017, 13, 1701354.
[31] Yang, H.; Chen, H.; Lin, W.; Zhang, Z.; Weng, M.; Zhou, W.; Fan, H.; Fu, J., Facile Preparation of Oxygen-Vacancy-Mediated Mn_3O_4 for Catalytic Transfer Hydrogenation of Furfural. Ind. Eng. Chem. Res. 2021, 60, 9706.
[32] Bao, J.; Zhang, X.; Fan, B.; Zhang, J.; Zhou, M.; Yang, W.; Hu, X.; Wang, H.; Pan, B.; Xie, Y., Ultrathin Spinel-Structured Nanosheets Rich in Oxygen Deficiencies for Enhanced Electrocatalytic Water Oxidation. Angew Chem Int Ed Engl 2015, 54, 7399.
[33] Zhuang, L.; Ge, L.; Yang, Y.; Li, M.; Jia, Y.; Yao, X.; Zhu, Z., Ultrathin Iron-Cobalt Oxide Nanosheets with Abundant Oxygen Vacancies for the Oxygen Evolution Reaction. Adv. Mater. 2017, 29, 1606793.

Acknowledgement Page

Instructor-Student Relationships and Contributions

1. Instructor-student relationship

Ms. Yuning Zhang, the chemistry teacher who taught us at our school, was responsible for guiding the design and implementation of our entire research project. Since the topic selection stage of our research, Ms. Zhang has given us great support and help. As an experienced researcher, Ms. Zhang shared with us the cutting-edge knowledge in the current field.

Ms. Zhang's guidance was not only limited to the topic selection stage. Throughout the whole research process, Ms. Zhang provided us with valuable suggestions, whether it was the optimization of experimental design or the methods of data analysis. She also helped us to solve various technical difficulties encountered during the experimental process, such as the data anomalies encountered in the sample characterization, Ms. Zhang gave us timely explanations and suggested us to adjust the experimental parameters.

2. The role of the instructor in thesis writing

In the dissertation writing stage, Ms. Zhang's role was equally indispensable. She not only assisted us in organizing our research ideas, but also gave us detailed guidance on the logical structure and language expression of the article. After the completion of the first draft, Ms. Zhang conducted a comprehensive review of the paper and made several suggestions for revision, especially optimizing the precision and professionalism of the language. Finally, Ms. Zhang also helped us to check all the experimental data to ensure the scientificity and rigor of the paper.

Overall, Ms. Yuning Zhang played a crucial role in the whole research process, and her unpaid guidance and support enabled our study to proceed smoothly and achieve satisfactory results.

3. Curriculum vitae of instructors

Yuning Zhang is currently a chemistry teacher at Haidian Kaiwen School in Beijing. She graduated from Tsinghua University with a Bachelor’s Degree in Basic Science and received her PhD in Chemistry and Biology from New York University. During her stay in the U.S., she taught core science and math courses to U.S. undergraduates and has more than ten years of teaching experience in high schools and universities. She has taught several high school science courses such as AP/A level Chemistry at Haidian Kaiwen School in Beijing and has been certified as an AP Teaching Experienced Teacher by the University Council of the U.S.A.; and is an excellent instructor in the UK and U.S. High Schools' International Chemistry Competitions (UKCHO, CCO).

Description of the Division of Labor for the Study

1. Sources of selection

The topic chosen for our study was derived from news reports that emphasized the significant impact of organic pollutants, especially industrial dye wastewater, on environmental quality and water resources. Large quantities of dye wastewater generated during industrial production, containing undecomposed dye molecules and other organic pollutants, pose a serious threat to soil and groundwater systems. We learned from reviewing relevant literature that existing wastewater treatment technologies have some limitations, such as low treatment efficiency and high energy consumption. Therefore, the team decided to investigate a new catalyst material aimed at enhancing the degradation efficiency of organic pollutants. After discussion with Zhang, we determined a research direction based on iron oxide (Fe_2O_3) nanofibers, focusing on exploring the catalytic degradation performance of organic dyes (e.g., methylene blue and rhodamine B) with oxygen vacancy defects on their surfaces.

2. Data acquisition and experimental design

The experimental design is partly based on references, especially the synthesis method of iron oxide nanofibers. We firstly synthesized iron oxide nanofibers using electrospinning and high temperature calcination, and then constructed oxygen vacancy defects on their surfaces by $NaBH_4$ reduction. The preliminary design of the experiment includes the following steps:

- Fiber synthesis: We prepared a stable electrostatic spinning solution by mixing $Fe(acac)_3$, polyacrylonitrile (PAN), and N,N-dimethylformamide (DMF), which was heated and stirred in an oil bath.
- Defect construction: oxygen vacancy defects were constructed on the fiber surface using $NaBH_4$ reduction to enhance its catalytic properties.
- Experimental optimization: After several experiments, we optimized the voltage, collection distance, temperature and humidity control parameters of the electrostatic spinning according to the suggestions of our supervisor, and finally determined the best experimental conditions. All experimental steps were performed in strict accordance with standard operating procedures to ensure the accuracy and reproducibility of the data.

After review and several discussions with our school instructors, we finalized the experimental design and decided to use methylene blue and rhodamine B as target pollutants for organic dye degradation in subsequent experiments.

3. Experimental implementation and data analysis

The experiments were carried out by Yijing Liu and Yingying Ma. Yingying Ma was responsible for sample preparation, which included experiments on the synthesis of iron oxide nanofibers, including the precise control of solution preparation during electrospinning and the setting of high temperature calcination conditions. She learned the spinning skills, and subsequently, she was also responsible for the experiments on the introduction of oxygen vacancy defects to adjust

the structure of the fiber surface by $NaBH_4$ reduction reaction. She synthesized iron oxide nanofibers strictly according to the literature and successfully introduced oxygen vacancy defects. In addition, Yingying Ma and Yijing Liu completed the degradation test of organic dyes and measured the degradation rate by spectrophotometer and organized the data and plotted the rate graph.

Yijing Liu was responsible for the structural characterization and data analysis of the experimental samples. Test characterizations such as SEM, TEM, XRD, EPR, XPS and N2 absorption desorption curves were mainly performed by third-party testing organizations such as Science Compass, and then he analyzed the morphology of the nanofibers by SEM and TEM results, confirmed the crystal structure by XRD, and oxygen vacancy defects by EPR and XPS. analyzed, and also tested the pore size distribution of the material by physical adsorption (N2 adsorption and desorption curves). Yingying Ma was the assistant. Meanwhile, he and Yingying Ma recorded the experimental data together, and discussed and analyzed the experimental results.

The two worked together to create the charts in the paper.

4. Writing and proofreading of papers

Writing: The writing of the thesis was done by Yijing Liu and Yingying Ma. Yijing Liu was responsible for writing and translating the abstract, preface, and experimental sections of the paper. The preface describes the environmental impact of organic dye wastewater, the limitations of current treatment methods, and the application of iron oxide nanofibers in catalysis; the experimental section describes the synthesis and characterization of the nanofibers. Yingying Ma was responsible for the results and discussion section. She analyzed the experimental results in detail, especially the enhancement of the catalytic performance by oxygen vacancies, and explained the results comprehensively with graphs and charts. She was also responsible for the conclusion section of the paper, which summarizes the main findings and contributions of the study.

Proofreading: After the first draft of the paper was completed, Liu Yijing and Ma Yingying worked together to check and revise the paper in detail, to ensure that the logic of the paper was clear, the data was accurate, and the language expression was fluent. In the end, the supervisor, Zhang Yuning, reviewed and optimized the paper, especially in the language and structure, and provided valuable suggestions to ensure that the paper met the requirements for publication.

5. Difficulties encountered and solutions

During our experiments, we encountered several challenges, including:

- Challenges in material synthesis: In the initial experiments, fiber breakage and uneven morphology occurred during the electrostatic spinning process. By adjusting the parameters of electrostatic spinning voltage, collection distance and ambient humidity, we finally succeeded in obtaining structurally homogeneous iron oxide nanofibers.

- Inconsistency of characterization data: At the beginning of EPR and XPS tests, the data fluctuated greatly due to improper sample handling. After many experimental repetitions and equipment debugging, we ensured the stability and accuracy of the experimental data.
- Differences in degradation experiment results: In the catalytic degradation experiment, we found that the defect-free iron oxides were significantly less efficient than methylene blue in degrading rhodamine B. The results of the degradation experiment showed that the defect-free iron oxides were significantly less efficient than methylene blue. We adjusted the experimental program after literature research and data comparison, and finally verified that the presence of oxygen vacancy defects did significantly enhance the catalyst activity.

6. Conclusion

Through the team's joint efforts, we successfully synthesized iron oxide nanofibers with oxygen vacancy defects and verified their efficient performance in the catalytic degradation of organic pollutants. The experimental results show that the oxygen vacancy defects play a crucial role in improving the catalytic efficiency. This study not only provides a new idea for the structural design of iron oxide nanofibers, but also lays the foundation for the design of catalysts in environmental pollution control in the future.